Rapport BIPM-83/4

# OPERATING CHARACTERISTICS OF TWO MAGNETIC SUSPENSION SYSTEMS

George T. Gillies

1983

Bureau International des Poids et Mesures

F-92310 Sèvres, France

TABLE OF CONTENTS

# Operating characteristics of two magnetic suspension systems

George T. Gillies
1983

Bureau International des Poids et Mesures
Pavillon de Breteuil
F-92310 Sèvres, France

## Abstract

Two identical magnetic suspension systems have been built and tested at the BIPM laboratories. These prototype instruments are easy to operate and stably suspend masses up to 500 grams without auxiliary magnets. The details of their construction and an analysis of their performance are given here, along with some discussion of their possible applications.

## Introduction

This paper is essentially a service manual for the optically sensed magnetic suspensions which have been built at BIPM. Sufficient detail is given for the relatively simple tasks of suspension startup, shutdown, and maintenance to be performed with ease. In fact, these suspensions are purposely simple in their design, giving the user great flexibility in terms of incorporating them into new or existing measurement systems.

These suspensions are nearly identical to those developed by Jones (1), Cheung (2), Leyh (3), Cheung, et al. (4), and (to some extent) Gillies (5) all at the University of Virginia. References (1-5) contain extensive technical documentation on the operation of magnetic suspension systems in general, and should be consulted by the reader for advice when planning improvements to or changes in the existing BIPM devices. They also present the theory of operation of magnetic suspension systems in a sufficiently general way that the details of the system models can be applied directly to the BIPM suspensions.

Figure 1, taken in modified form from (1), shows the principle of operation of the BIPM suspension systems. Light from an LED, $D_1$, is collimated by lens $L_1$ and passed under the pole-piece M of the electromagnet coil C. Depending on the diameter of the cross section of the light beam, one may or may not use a second lens $L_2$ to focus it on to the active area of the split-cell photodetector $D_2$. In the BIPM suspensions, the lens $L_2$ is not used. The photocurrents of $D_2$ are proportional to the displacement of the suspended body, typically a ferromagnetic sphere which is in the center of the light beam. The

differential pre-amplifier produces a voltage proportional to the photocurrents, and this signal drives the power amplifier $A_2$. The electromagnet current, supplied by $A_2$, is always such as to produce only the exact amount of magnetomotive force necessary to balance the gravitational force on the test body and produce stable suspension. The stabilizing phase lag is produced by an active differentiator.

The mechanical, optical and electronic construction details are given below.

## Mechanical Structure

Figure 2 is a photograph of the BIPM-1 system in operation. The mechanical construction is straightforward. A Plexiglass (Perspex) plate, 72 cm × 21 cm × 1.5 cm, serves as the mounting for the servocoil (electromagnet). This rectangular plate is supported by four aluminium legs, one at each corner. The legs are 1 cm in diameter and 27 cm long, and are fixed to brass rails supported by anti-skid rubber feet. Aluminium angle brackets have been added to the corners to stiffen the framework and prevent sagging or bowing caused by the weight of the servocoil.

No special provisions have been provided for either tilt control or vibration isolation, although future experiments with refined versions of these devices would need such improvements.

Plexiglass was chosen for the mounting frame (and for the servocoil winding form) because it is electrically non-conducting yet mechanically stiff. One must avoid having closed loops of conducting material around the servocoil since the resultant eddy current losses would reduce substantially the suspension's efficiency.

## Electro-optical System

Considerable experience with single-cell photodetectors used as suspended-body position sensors (5) led to the conclusion that much more stable support can be expected with split-cell detectors. For instance, single-cell detectors have a temperature drift as large as that of carbon composition resistors, and external compensating circuitry must be used to eliminate the drift.

In general, the inherent common-mode rejection of split-cell detectors makes it possible to operate a suspension in daylight, artificial light, and darkness ; even under conditions of large ambient temperature changes.

The specific detector used in these suspension systems is the Silicon Detector Corporation "Quadrant Detector", Model SD-380-23-21-051. Appendix I contains the manufacturer's data sheets for this detector. An alternative detector with nearly identical specifications is the United Detector Technology Corp. Model PIN-Spot/9D, the data sheets for which are in Appendix II.

Figure 3 shows the schematic diagram for the detector-pre-amplifier - as well as for the rest of the suspension circuitry, discussed later. The four independent photodiode anodes are joined electrically into two pairs and each pair is connected to the inverting input of a low noise LM308AN operational amplifier. One of these amplifiers has a fixed feedback resistor and the other has a variable resistor. In order to balance the system, the output voltages of both of these amplifiers are measured simultaneously while the entire surface of the photodiode is illuminated by a dc light source. The light must not be too bright, or the photodiodes will saturate electrically.* Under these conditions, the variable resistor is adjusted such that the two outputs are equal to within 1.0 mV. The detector-pre-amplifier is now balanced electrically, and when these two signals are "differenced" by the next operational amplifier, all modes common to both will be subtracted. Therefore, 50 Hz hum, 100 Hz fluorescent-light noise, and all other common-mode signals do not get passed into the remaining signal handling stages.

In practice, the detection system's light beam should be produced by a stable, efficient source. Some applications call for a light beam with low energy density so that the test mass is not heated appreciably when irradiated. Convenient for this purpose are standard LED indicator lamps. Red lamps are most frequently used since the spectral response of silicon photodetectors, such as those discussed above, increases with wavelength into the near infrared. In order to ensure adequate uniformity of the light density over the entire cross-section of the LED output beam (after collimation), one typically alters the LED package in the way described in Appendix III. Power for the LED is taken from one of the ± 15 Vdc operational amplifier power supplies, and a 500 Ω, 5 W current-limiting resistor is put in series with it. Under these conditions, a current of 30 mA flows through the LED. This is about the maximum level permissible ; beyond this the LED semiconductor junctions can be irreversibly damaged. One can use higher currents and therefore increase the LED brightness but only if the higher levels of current are delivered in pulses of short duty-cycle.

The LED beam is collimated by a double convex lens of diameter 17.5 mm and focal length 39 mm in one system ; and by a double convex lens 20 mm in diameter and 34.5 mm in focal length in the other. [The only reason for using non-identical lenses was that two identical ones were not readily available at the time of construction.] The LED is positioned at an object distance equal to the focal length of the lens in order to collimate its light beam. The beam diameter upon exiting the lens depends upon exact adjustment, but is usually about 15 mm. With beams this small, no second lens is necessary. This is because the suspended bodies typically used are small enough not to interrupt all the light when the suspension is operated in the "balanced" mode, and other, larger bodies can be suspended in the "semi-balanced" mode which uses only half of the light beam. The details of these two operating modes are discussed later.

---

*The system is saturated when the operational amplifier outputs equal their supply voltages, which are nominally ± 15 Vdc.

The photodetector/pre-amplifier is housed in an aluminium cylinder which also serves as a grounded shield for the circuitry it contains. The pre-amplifier output is connected to the rest of the electronics via a BNC cable.

The LED is housed in a teflon tube which also contains the current-limiting resistor. This tube telescopes into a second teflon tube at the front of which the collimating lens is fixed. By moving the LED tube inside of the lens tube one can adjust the beam collimation and size to the optimal value for any particular application.

Figure 4 shows these tubes and their cabling alongside a scale in centimetres.

Both the detector tube and the LED/lens tube are held inside circular ring clamps whose rods pass through brass fixtures mounted on the Plexiglass plate. In this way, adjustments of both vertical and azimuthal positions can be made.

## Electronic Circuitry

The remaining part of the electronic circuitry is quite standard and has been described in detail (1, 2, 3, 5). Nevertheless, a discussion of the principal features of the circuitry is given below.

The detector/pre-amplifier circuit is mounted on Vero board and surrounded by a Teflon sheet which prevents electrical contact with the inside wall of its aluminium housing tube. The rest of the suspension circuitry, except for the stand-alone power amplifier, is housed in an aluminium mini-box.

From stage to stage, the circuit elements in the mini-box are the following : (1) a switchable inverting/non-inverting amplifier which controls the sense of the feedback, (2) a gain stage which controls the system's proportional gain, (3) an offset amplifier which controls the system's dc level, (4) an active differentiator which damps vertical oscillations of the suspended body and (5) a voltage follower which presents a constant output impedance (and no varying phase shifts) to the power amplifier.

The phase of the output signal can be changed by 180° with respect to that of the input signal by throwing the switch on the mini-box control panel from "Inv" to "NonInv". By doing so, one changes the polarity of the output of the unity-gain operational amplifier preceding the gain stage, as mentioned above. This adds flexibility to the circuit and permits one to use power amplifiers different from the one discussed below, if necessary.

The gain stage is regulated by adjusting a 10-turn potentiometer on the mini-box front panel, as is the offset amplifier. When the counting dial of the offset amplifier is set at 5.00, it adds no dc to the system's signal level.

The details of the differentiator are given by Gillies in reference (5).

All operational amplifiers in the pre-amplifier network and the signal-handling network contained in the minibox are powered by Analog Devices Corp. Model 920E dual-output (± 15 Vdc) power supplies (200 mA maximum).

All adjustable resistors are ten-turn wire-wound potentiometers. They have full-range linearity better than 0.25 %, and retain this linearity unless they are used to dissipate large amounts of power.

The LM308AN operational amplifiers used in the pre-amplifier are externally compensated by 20 pF capacitors in order to filter high-frequency ringing from the signal. The other operational amplifiers are all standard internally-compensated RCA Corp. Model CA741CE.

The power amplifier is a Kepco Corp. Model BOP 36-6M bipolar operational power supply/amplifier. This unit can drive from 0 to ± 36 V at from 0 to ± 6 A over a frequency range of dc to ≈ 1.5 kHz. It is operated in the "voltage" mode (the voltage control switch "on" and the current control switch "off").

The front-panel connections on the power amplifier are as follows : The output from the voltage follower, the last stage of the operational amplifier circuitry in the mini-box, is used to drive the power amplifier's "voltage programming input" via BNC cable. The black "common" jack is linked to the black "sense" jack, and the red "output" jack is linked to the red "sense" jack. The green "ground" jack is left unconnected. The servocoil connections are made by putting banana plugs on the coil leads and inserting them into the "output" and "common" jacks. The front-panel "voltage control" potentiometer serves only to add dc offset onto the signal, and is therefore redundant with the offset control in the operational amplifier circuitry. It may be adjusted if convenient ; it is preferable to leave it zeroed.

The servocoil consists of approximately 4,700 turns of 0.8 mm diameter, enamelled copper wire wound on a Plexiglass (Perspex) coil form whose inner diameter, with no windings present, is 12 mm and whose outer diameter (when fully wound) is ≈ 100 mm. The length of the coil is about 100 mm. The coil core is made of cold-rolled steel 10 mm in diameter, 177 mm long with a hemispherical pole-piece. It is held in place by nylon bushings with brass scews. The coil resistance at dc is 33.6 Ω, and it has an inductance (with core) of 0.85 H. Its impedance at 500 Hz is about 2 700 Ω.

Figure 5 shows a plot of the frequency response of the electronic part of the system in the critical (low audio) range necessary for stable suspension. It shows the typical high-frequency enhancement associated with active differentiators. A roll-off, however, occurs at about 1.7 kHz due to the limited frequency response of the power amplifier.

## Operating Suggestions and Trouble-shooting Procedure

These suspensions can be operated under almost any ambient light and temperature conditions. Direct illumination of the photodetector by bright light, though, will saturate the pre-amplifier. This must be avoided.

The first step in achieving successful operation involves checking the alignment of the optics. The collimated beam exiting from the LED/lens tube should be circular in cross-section and should fall directly on the active area of the photodetector.

The top of the beam should be no more than about 12 mm below the bottom of the coil's pole-piece. This dimension is not critical, but in general the larger the pole-piece/rotor separation, the larger the coil-current needed for stable support. On the other hand, large coil-currents (say, greater than 1.0 A) lead to ohmic losses in excess of 20 W in the servocoil, and this, too, should be avoided.

The gain setting on the feedback circuitry determines the speed of response of the system. Typically, one should use as large a gain as possible in order to minimize drift in the rotor height.

Vertical oscillation of the rotor will result, though, from either too high a gain setting or from too much dc offset. If oscillations begin, one should lower the offset rather than lower the gain. Sometimes it is necessary to lower both, particularly if small rotors are to be suspended.

Initiating the suspension (putting the rotor into support) is often the most difficult part of the process. One must be careful to minimize the amount of light interrupted by one's fingers while holding the rotor in the light beam. It is necessary to manipulate the offset control and the rotor simultaneously in order to obtain stable support.

With a little experience, one can feel the rotor "lock into" the stable support region yet, when released, it usually starts to oscillate violently and often falls. One must simply spend time manipulating the gain and offset controls in order to arrive at the right combination for any given rotor. Complete inability to gain stable support usually means that either the optical system has become misaligned or that the "Inv" - "Noninv" switch must be thrown. However, once in support, should the rotor fall because of mechanical shock or accidental interruption of the light beam, it is usually possible to simply place it back in support without changing the controls. Note, too, that drifts may occur during the first two or three hours of operation due to warm-up by ohmic heating of the servocoil. This is easily compensated by changing the offset as necessary.

It should be noted that there are, in theory, two points of stable support for all rotors. These correspond to 1) rotor positions where the rotor shadow falls on only the bottom half of the photodetector (the "semi-balanced" mode), and 2) rotor positions where the rotor shadow is

geometrically centered on the photodetector (the "balanced" mode). The BIPM systems operate in mode 1 but, with changes to the optical system, could be made to operate in mode 2. Even operating "semi-balanced", though, the common-mode rejection available makes it a far more stable type of support than that achievable with single-ended photodiodes.

When closing down a suspension, one simply removes the rotor from support. Before turning off the power amplifier, however, one must adjust the offset control so that the coil-current is brought to zero. If this is not done, the collapse of the magnetic field of the servocoil produces a very large voltage which will damage the output stage of the power amplifier, necessitating expensive repairs. This damage mechanism is known as "inductive kick". While it is not severe for coil currents of a few mA, it can be for higher current levels ; and it is therefore highly recommended that the above shut-down procedure be followed.

The trouble-shooting procedure for these systems is straightforward. If stable support cannot be achieved, do the following :

(A) Check the alignment of the optical system. See that the light beam passes under the center of the coil pole-piece and that it falls symmetrically on the photodetector.

(B) Try changing the phase of the feedback by 180° using the "Inv" - "Noninv" switch.

(C) Check the photodetector output to be sure that it is not saturated. If it is, reduce the level of ambient light or put some black paper around the fronts of the LED/lens and detector tubes. This will help to screen out ambient light.

(D) Check the operational amplifiers in the pre-amplifier and feedback networks for "shorts", open circuits or other failures.

(E) Check the operational characteristics of the Kepco power amplifier, following the procedures outlined in its service manual.

The above steps should isolate the problem, and the corrections needed will usually be obvious. Please note, too, that one should verify the continuity of all cables. Further, the voltage levels of the ± 15 V dc supplies should be checked under load, as quite frequently nothing more serious than power supply failure is at the root of such problems. Occasionally, more subtle difficulties develop, and can be dealt with by referring to references (1-5). The author's experience, though, is that optical misalignment is usually the source of trouble.

## Performance Characteristics

The BIPM-1 suspension has had over 350 hours of maintenance-free operation, including one uninterrupted stretch of about 100 hours wherein the rotor-height variation was probably much less than one

wavelength of light. Interferometric measurements of ultimate stability have not yet been made.

Figure 6 shows a solid steel rotor of about 100 g mass in suspension, and Figure 7 a cylindrical rotor of about equal mass. Other shapes can be suspended, too, but for highly irregular geometries it is usually best to attach a small ferromagnetic sphere by a thin extension rod and let this act as the sensed mass (cf., reference 1).

The principal forces at work in the vertical direction are the gravitational, buoyancy and magnetic forces, the first being balanced by the last two, evidently to better than 1 part in $10^6$ over a one second averaging time. There are also torques about the suspension axis and in some applications these must be made very small. Such torques arise from the interaction between the residual magnetic moment in the ferromagnetic rotor and the azimuthal gradient of the magnetic field. In principle, these can both be made very small by annealing the rotor and by careful design of the servocoil. In practice, restoring torque constants as small as $7 \times 10^{-10}$ N m have been observed although, at this level, the stability of the rotor's residual magnetic moment is not good and the value of the restoring torque drifts.

## Applications : Proposed Experiments

These instruments are prototypes which are adaptable to a variety of different uses. A few possibilities will be mentioned here.

A. Sakuma has proposed the use of a suspended body as a new type of seismometer. The feedback signal contains complete information on the displacement, velocity and acceleration of the rotor with respect to the surface of the earth, and spectral analysis of it would produce a substantial amount of information on both natural and man-made vibrations. Problems associated with using a suspension in this way might arise from errors in the repeatability of rotor positioning, residual drifts due to power supply output variations and dc tilts of the suspension framework.

T. Quinn has proposed the use of a suspension system as a feedback mechanism for a flexure strip balance. Difficulties to be overcome here include mechanical drift, non-negligible magnetic susceptibilities in the kilogram prototypes, differential thermal expansion and low frequency oscillations on the feedback signal.

T. Witt has proposed the use of a suspended rotor as the indicator in a novel galvanometer system. In this case, some limiting factors might be instability of the azimuthal restoring torque (especially at low torque levels), vertical-position/azimuthal-angle-offset couplings, and non-linearities in the torque produced by the drive coils at highest sensitivities.

## Applications : Experiments in Progress

Two other experiments have been initiated with these systems, although neither is far advanced as yet. Their principles of operation are discussed below anyway.

### Laser Power Meter

Increases in the sensitivity and accuracy of absolute laser-power measurements at the milliwatt level would be welcome. With this in mind, the radiation pressure technique of Aida and Bouzidi (6) was re-examined with the goal in mind of replacing the fiber suspension of their movable mirror by a magnetic suspension. The preliminary apparatus developed for this purpose was designed following their apparatus and it is shown in operation in Figure 8. The principle of the method is very simple. The inverted "T" has a mirror of high, known reflectance on one arm and a counterweight (an identical mirror) on the other arm. When a laser beam is reflected from the mirror at near normal incidence while the entire mechanism is magnetically suspended (as shown in Figure 8), a couple acts on the system about its suspension axis and the system rotates through a small angle. From a measurement of this angle and the intrinsic suspension restoring force, together with a knowledge of the rotation-axis/laser-beam spacing, the laser output power can be deduced. Problems with this technique include accounting for radiometric forces, heating of the irradiated mirror (with resulting thermal expansion) and the absolute measurement of the rotation axis/laser-beam spacing.

### Low-Frequency Vibration Isolator

A second experiment involved the suspension of a two-mass mechanical oscillator. Figure 9 shows two steel spheres, with one of them magnetically suspended and the second mechanically suspended by the spring from the first. With respect to the suspension framework, i.e., the earth, the lower sphere is coupled by two springs, the first mechanical and the second magnetic. The point of this exercise was to create the basis for an improved "super spring". That is, an ultra-low-frequency vibration-isolation system, such as that developed by Rinker and Faller (7). In this case, though, rather than using a suspended loud-speaker coil to drive the mechanical spring, we isolate and drive the mechanical spring by magnetic suspension. This has the advantage of tuneability, that is, one can change the "upper" spring constant merely by changing the gain, with the result that perhaps even sub-microseismic noise can be isolated.

Although both of the above-mentioned mechanisms were made operational, much additional work will be required in order to make these devices useful tools.

## Conclusions

Two identical magnetic suspension systems have been built, tested and are now available for use at the BIPM. Their operating characteristics have been presented and discussed. Possible applications have been mentioned and limiting factors for each of them suggested.

Although the designs for these instruments are not inherently new, they do have some novel features which should make them useful as a new type of metrological tool.

## Acknowledgements

I thank Mr. Georges Boutin for assistance with the mechanical construction, and Dr. Terry Quinn for many useful discussions.

## References

1. JONES, G.R., Jr. Decay time studies of magnetically suspended rotors. M.S. Thesis, University of Virginia, 1981, 111 pp.

2. CHEUNG, W.-K.S. Servo driven corotation : development of an inertial clock. Ph.D. Thesis, University of Virginia, 1982, 300 pp.

3. LEYH, C.H. The development of an oscillating sphere viscometer. M.S. Thesis, University of Virginia, 1981, 74 pp.

4. CHEUNG, Wah-Kwan Stephen, GILLIES, George T., LEYH, Carl H., and RITTER, Rogers C. Ultra-stable magnetic suspensions for rotors in gravity experiments. Prec. Engng., 2 1980 : 183-186.

5. GILLIES, G.T. The development of high Q, precision mechanical rotors for use in a dynamic measurement of matter creation. Ph.D. Thesis, University of Virginia, 1980, 141 pp.

6. AIDA, Y. and BOUZIDI, M. Radiation pressure measuring methods for the determination of He-Ne laser beam power. IEEE Catalogue, 80CH 1497-71M 1980 : 269.

7. RINKER, R.L. and FALLER, J.E. Long period mechanical vibration isolator. In : Precision Measurement and Fundamental Constants II, edited by B.N. Taylor and W.D. Phillips, National Bureau of Standards (U.S.) Special Publication 617, Washington, D.C., U.S. Printing Office, 1983, in press.

---

20/4/83

Appendix I

SILICON DETECTOR CORPORATION, 855 Lawrence Dr., Newbury Park, CA 91320, Phone:805/498-6737, Telex:182225

# POSITION SENSORS

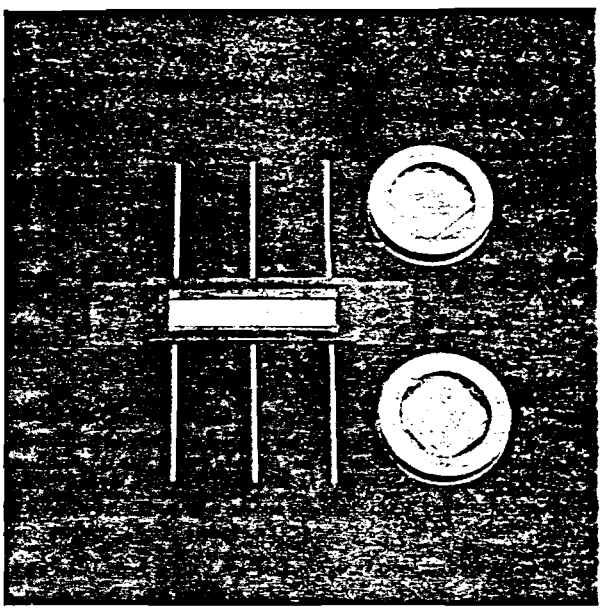

## GENERAL DESCRIPTION

SDC's Position Sensor group includes Lateral Cells and Segmented Detectors. These devices are used to precisely measure the location of optical images with respect to specified system reference points.

Lateral Cells are noted for their wide dynamic range. They achieve very accurate analog position measurement over relatively large areas. The response of these detectors is not influenced by the size or shape of the light image as long as this image remains within the active area of the detector. Moreover, operation far from the optical center or null point of the system does not impair accuracy. Lateral Cells are offered in both single-axis and dual-axis configurations.

Quadrant Detectors represent SDC's only current Segmented Detector offering. In most common applications Quadrant Detectors sense position deviations of a light spot about the optical axis of a system. Position measurement may be made over a range equal to the diameter of the light spot. Segmented Detectors are unsurpassed for detecting minute fluctuations near the null point and can operate at very high optical modulation frequencies.

## APPLICATIONS

- Vibration Analysis
- Optical "Bore-Sighting" and Alignment
- Measurement of Optical Aberrations and Distortion
- Angle Measurement and Indexing
- Non-Contact Surface Profiling

## CHARACTERISTICS

- Accurate Analog Position Measurement - ±.06 cm
- Detection of Minute Position Shifts - ±1 Angstrom
- Large Measurement Range -
  −.49 cm to +.49 cm (dual-axis)
  −1.48 cm to +1.48 cm (single-axis)
  .97 cm diameter (quad)
- Fast Pulse Response (quad) - 8 Nanoseconds
- High Peak Responsivity - 0.55 A/W

# OPERATING SPECIFICATIONS

| PARAMETER | Lateral Cells | | Quadrant Detectors |
|---|---|---|---|
| | SD-1166-21-11-391 | SD-386-22-21-251 | SD-380-23-21-XXX |
| Typical Peak Responsivity (A/W) | .50 | .55 | .55 |
| Maximum Nonuniformity of Response When Scanned with a 1mm Light Spot (%) | ±5 | ±5 | ±5 |
| Typical Position Sensitivity at Spectral Peak (A/cm) | .37P * | 1.1P * | .5 P/R * |
| Guaranteed Position Measurement Accuracy over Operating Range (cm) | ±.06 (Max) | ± .1 (Max) | ±.06R * For Uniform Spot |
| Minimum Detectable Position Change (Angstroms) | $10^{-3}\sqrt{\Delta f/P}$ * | $4\times10^{-4}\sqrt{\Delta f/P}$ * | $1.5\sqrt{\Delta f/H}$ * |
| Typical Thermal Drift of Null Point ( $\mu$m/°C) | 1 | 1 | $R\times10^{-5}$ * |
| Measurement Range (Active Area Size -cm) | −1.48 to +1.48 (single-axis) | −.49 to +.49 (dual-axis) | −R to +R * (dual-axis) |
| Dynamic Output Resistance - $R_D$ | 2kΩ (typ) | 1.5kΩ (typ) | 10MΩ (min) |
| Typical Parallel Output Capacitance - (pF) | | | |
| Junction Bias 0 Volts | 13,000 | 1500 | 300 |
| Junction Bias 5 Volts | 5,500 | 620 | 124 |
| Junction Bias 50 Volts | — | 240 | 48 |
| Maximum Dark Output Current - $I_d$ (nA) | | | |
| Junction Bias 5 Volts | 1000 | 1000 | 50 |
| Junction Bias 50 Volts | — | — | 140 |
| Maximum Light Modulation Frequency - Δf | | | |
| Junction Bias 0 Volts | 12kHz | 35kHz | 4MHz |
| Junction Bias 5 Volts | 28kHz | 85kHz | 10MHz |
| Junction Bias 50 Volts | — | 220kHz | 25MHz |
| Maximum Total Light Current (sum of outputs) | 100 $\mu$A | 100 $\mu$A | 10mA |
| Maximum Total Light Power on Device @ Spectral Peak-P(mW) | .20 | .18 | 18 |
| Maximum Light Power Density @ Specral Peak-H (mW/cm²) | 100 | 25 | 25 |

* R ≡ radius of light spot in cm
Δ f ≡ system bandwidth in Hz
P ≡ total light power on device in Watts
H ≡ power density in light spot in W/cm²

EQUIVALENT OUTPUT CIRCUIT: Each Output

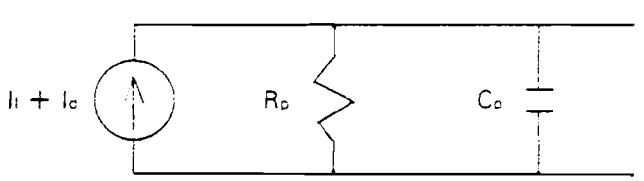

## TYPICAL CIRCUIT CONNECTION

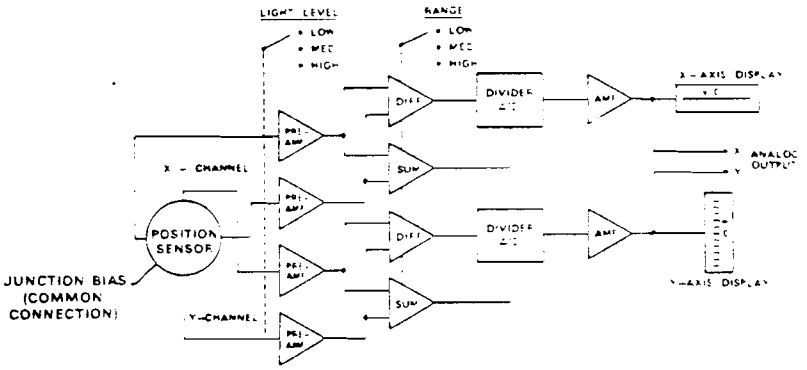


## OUTPUT TRANSFER CHARACTERISTIC (IDEAL)

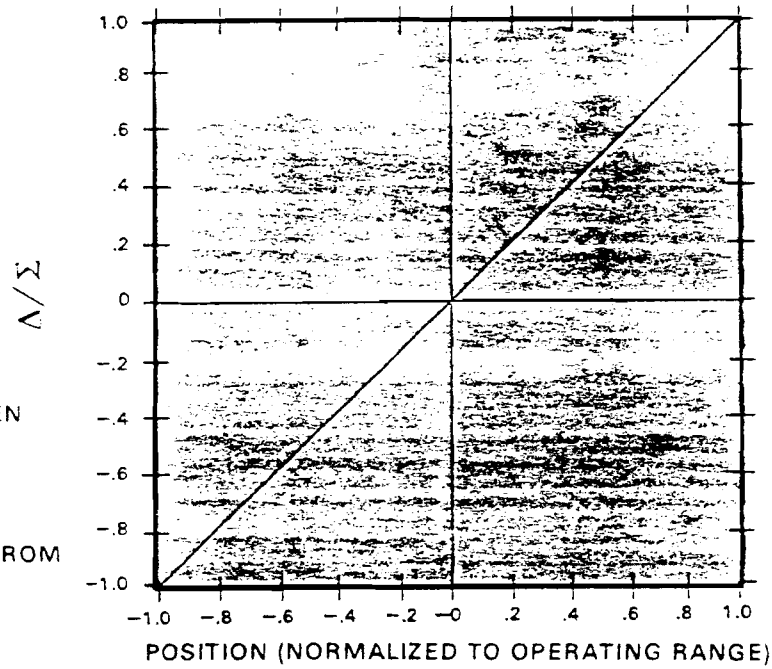


Δ ≡ DIFFERENCE BETWEEN CURRENTS FROM OPPOSING OUTPUTS

Σ ≡ SUM OF CURRENTS FROM OPPOSING OUTPUTS

## TYPICAL SPECTRAL RESPONSE (Photovoltaic @ 25° C)

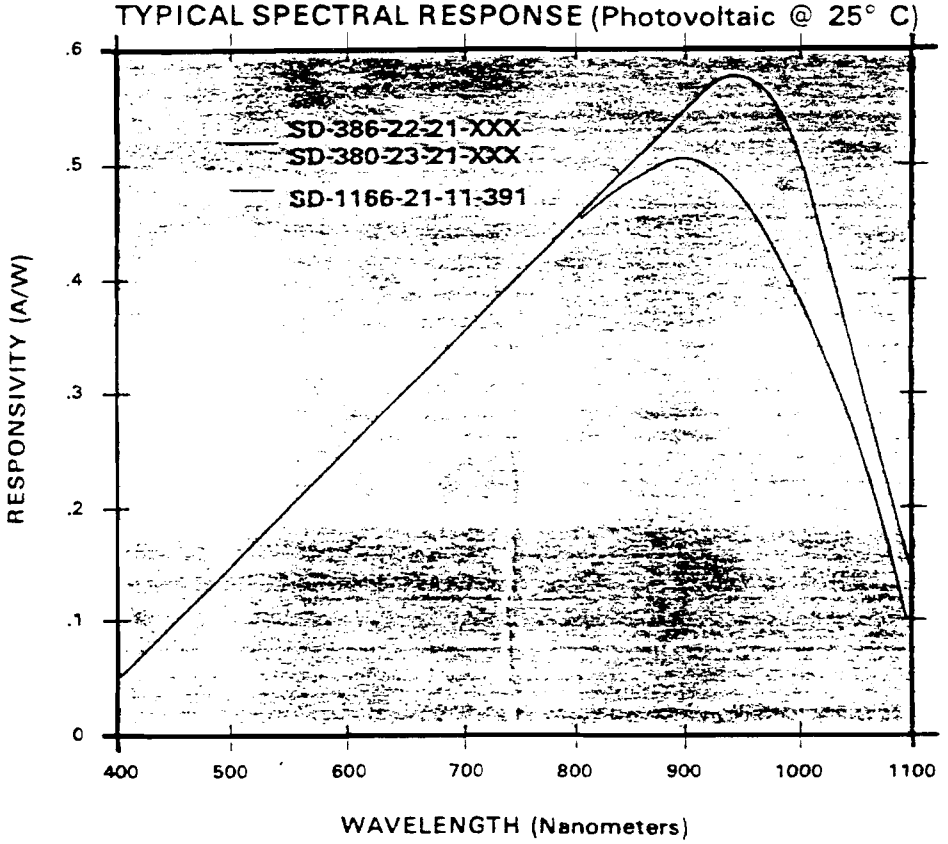

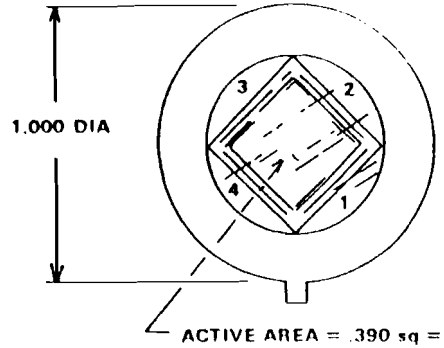


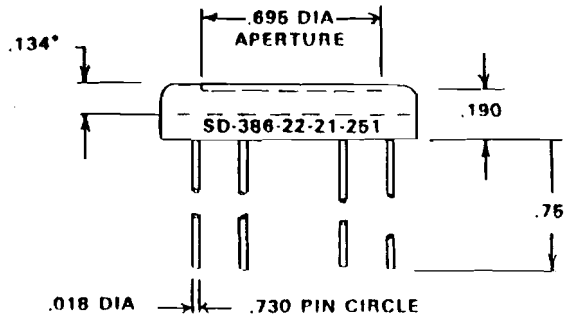


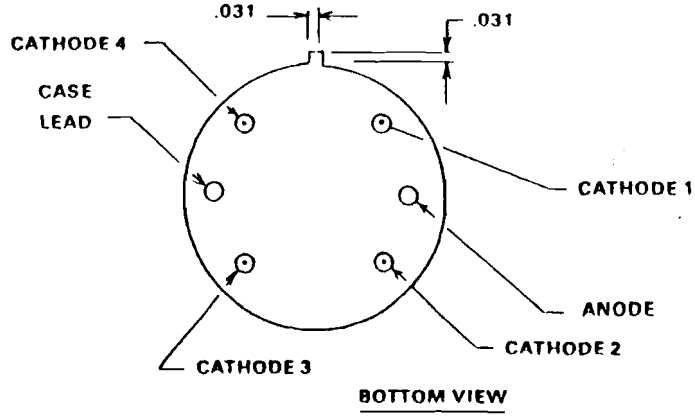


SD-386-22-21-251

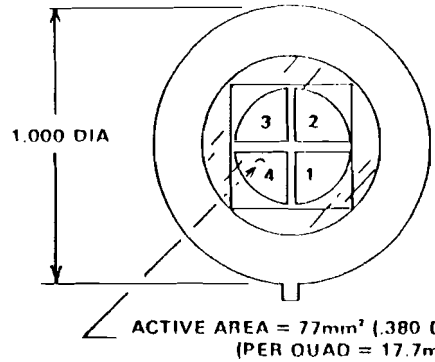


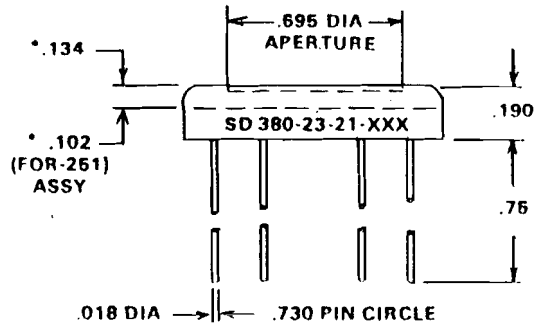


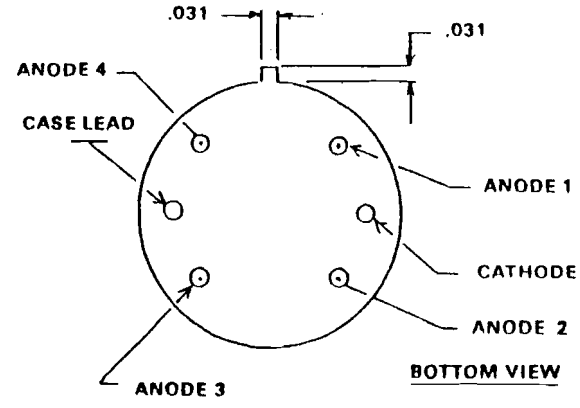


SD-380-23-21-051 (251)

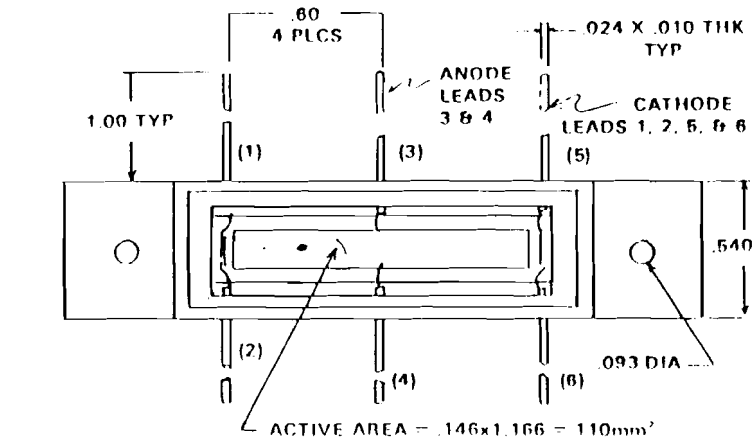


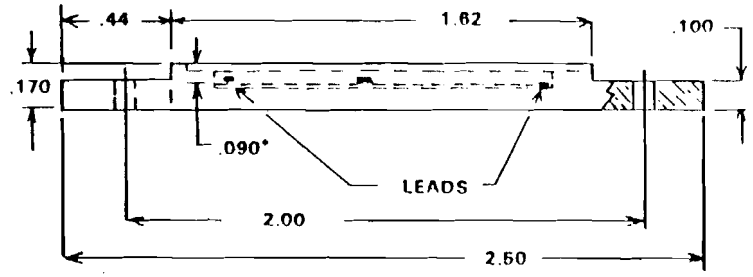


SD-1166-21-11-391

* DIMENSION FROM OUTSIDE OF WINDOW TO ACTIVE AREA OF PHOTODIODE.

SILICON DETECTOR CORPORATION

| | | |
|---|---|---|
| SCALE: FULL | APPROVED BY: | DRAWN BY T.M. |
| DATE: 9-22-77 | RMM/DLM | REVISED |

POSITION SENSOR DIMENSIONS

| | |
|---|---|
| B 400-44-003 | DRAWING NUMBER A |

POSITION SENSING DETECTORS
PIN Spot/8D, Spot/9D

# UNITED DETECTOR TECHNOLOGY, INC.

UDT's "Spot" series position sensors are bi-cell or quadrant detectors ideally suited for a wide range of nulling and centering applications.

The devices consist of two or four discrete elements on a single substrate with an active output lead from each element. When a light beam is centered on the detector (null or center position is the intersection of active elements) output current from each quadrant is equal. As the beam moves, current imbalance indicates off-center position. These devices exhibit excellent stability over time and temperature, high responsivity and fast response times necessary for pulse operation.

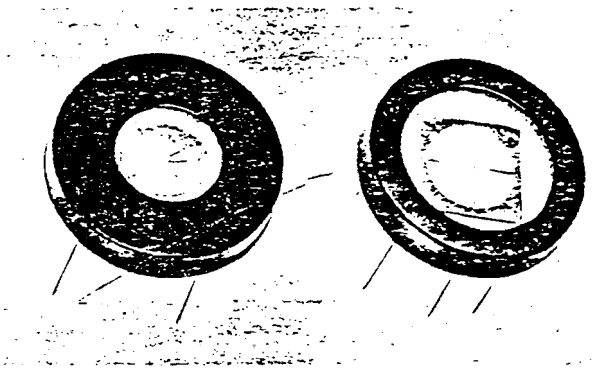

The PIN-Spot/8D and PIN-Spot/9D are quadrant detectors for two axis position information.

FEATURES:
Broad frequency response
Fast rise time
Low capacitance
High accuracy, long term stability of null position
Easy hookup

APPLICATIONS:
Lens centering
Feedback control systems
Guidance systems
Laser alignment
Machine tool alignment
Targeting
Process machinery alignment

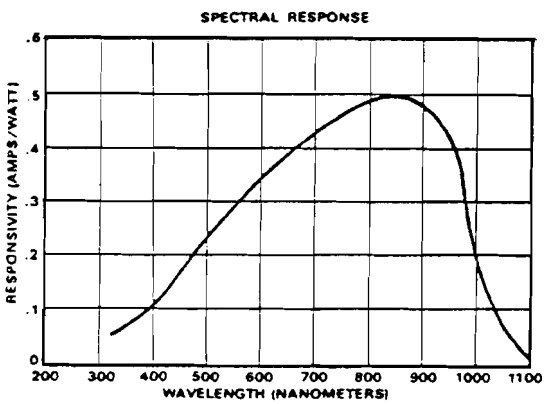


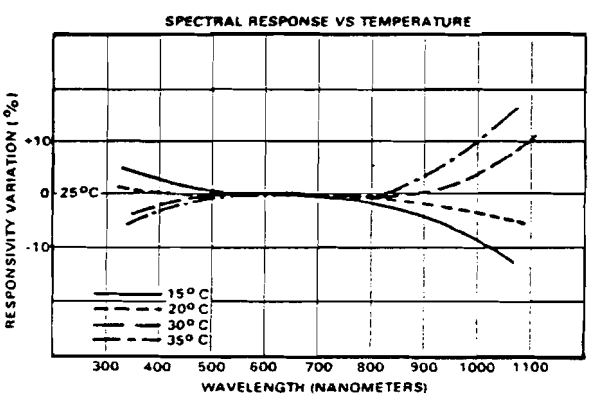


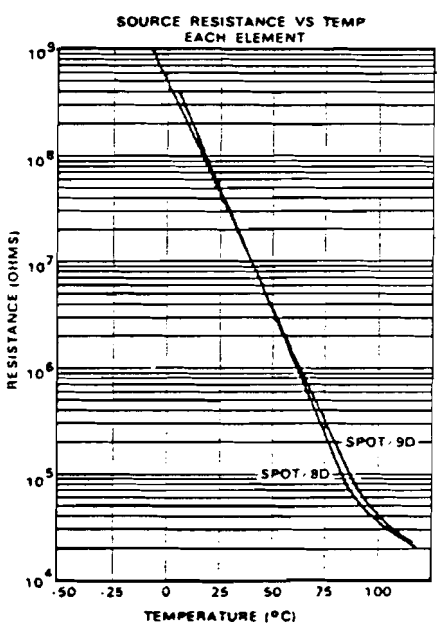


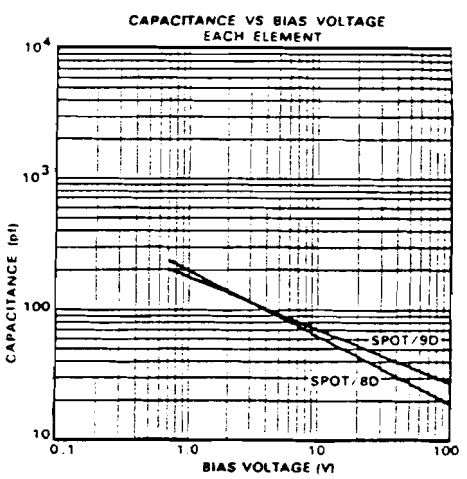


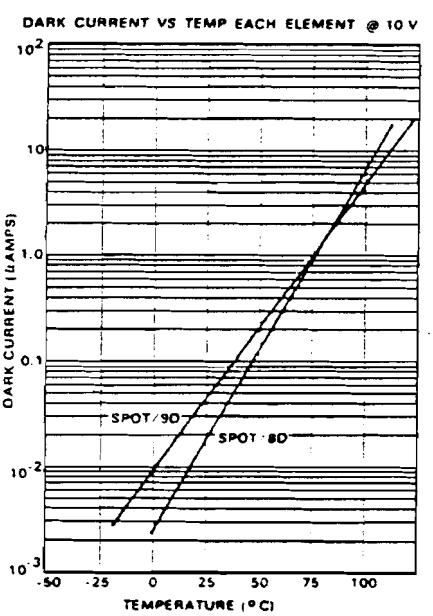


2644 30TH STREET, SANTA MONICA, CA 90405 ■ TELEPHONE (213) 396-3175 ■ TELEX 65-2413

## ELECTRICAL CHARACTERISTICS

| PARAMETER AND (UNITS) | | PIN-Spot/8D | | | PIN-Spot/9D | | |
|---|---|---|---|---|---|---|---|
| | | MIN | TYP | MAX | MIN | TYP | MAX |
| Recommended Mode of Operation | | Photoconductive/Photovoltaic | | | Photoconductive/Photovoltaic | | |
| Spectral Range @ 5% of Peak (nm) | | 350–1100 | | | 350–1100 | | |
| Responsivity at Peak λ (amps/watt) | | 0.4 | 0.5 | – | 0.4 | 0.5 | – |
| Uniformity of Response (with 1 mm spot dia) | | – | ±2% | ±5% | – | ±2% | ±5% |
| Dark Current Per Element (μa) | @ 10V Bias | – | 0.02 | 1.0 | – | 0.04 | 1.0 |
| Source Resistance Per Element (MΩ) | | – | 5 | – | – | 4 | – |
| Breakdown Voltage (volts) | @ $I_d$ < 100 μa | 50 | 100 | – | 50 | 100 | – |
| Capacitance Per Element (pF) | @ 0V Bias | – | 228 | 340 | – | 200 | 400 |
| | @ 10V Bias | – | 54 | 80 | – | 66 | 130 |
| | @ 50V Bias | – | 27 | 40 | – | 37 | 74 |
| Rise Time at 632.8 nm 10%–90% (ns) With 50-Ohm Load | @ 10V Bias | – | 15 | – | – | 15 | – |
| Fall Time at 632.8 nm 90%–10% (ns) | @ 10V Bias | – | 15 | – | – | 15 | 15 |
| Frequency Response at 632.8 nm (MHz) With 50-Ohm Load | @ 10V Bias | – | 10 | – | – | 10 | – |
| | @ 50V Bias | – | 10 | – | – | 10 | – |
| Maximum Output for 10% Nonlinearity (ma) | @ 10V Bias | 0.5 | 1.0 | – | 0.5 | 1.0 | – |
| NEP @ Peak λ, 1 kHz, 10V (w/Hz½) | | – | $2.5 \times 10^{-13}$ | – | – | $8.6 \times 10^{-13}$ | – |
| Forward Resistance (Ω) | | – | 100 | 600 | – | 100 | 600 |
| Approximate Saturation Level (mw) | | – | 10 | – | – | 10 | – |

## MECHANICAL SPECIFICATIONS

| SPECIFICATION | PIN-Spot/8D | PIN-Spot/9D |
|---|---|---|
| Active Area Total Area ($cm^2$) | 0.555 | 0.78 |
| Dimensions (in.) | 0.340 dia. | 0.394 dia. |
| Package Type | 1" Kovar | 5-Pin Header |
| Window | Glass | Glass |
| Field of View Full Angle | 122° | 145° |
| Temperature Range Operating (°C) | 0 to +75 | 0 to +75 |
| Storage (°C) | -25 to +75 | -25 to +75 |

## OUTLINE DIMENSIONS

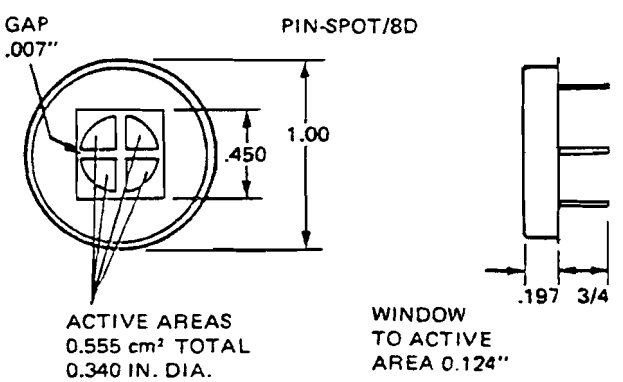


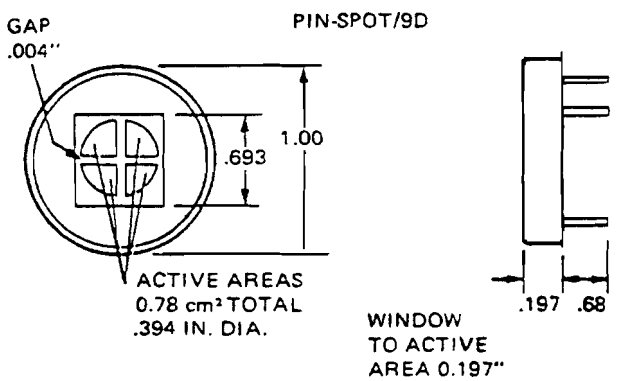


## SCHEMATIC DIAGRAM

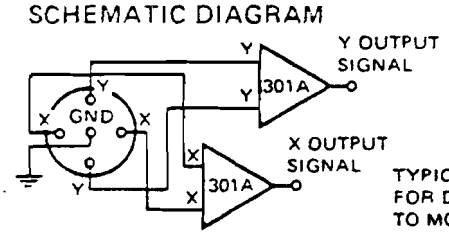


TYPICAL CONNECTIONS FOR DUAL AXIS DETECTOR TO MODIFIED UDT 301A AMPLIFIER*

*Amplifier bias polarity must be changed.

SPECIFICATIONS SUBJECT TO CHANGE WITHOUT NOTICE

D-018-0777

UNITED DETECTOR TECHNOLOGY, INC.
2644 30TH STREET, SANTA MONICA, CA 90405 ■ TELEPHONE (213) 396-3175 ■ TELEX 65-2413

418 Am. J. Phys. 48(5), May 1980 0002-9505/80/050418-02$00.50  

Appendix III

# Altered light-emitting diode point source emitter

George T. Gillies
*Physics Department, University of Virginia, Charlottesville, Virginia 22901*

It is often necessary to produce a collimated light beam in the student laboratory for use in optics experiments. There are several ways of doing this, such as expanding a laser beam or collimating incandescent lamp light.

There are, however, general disadvantages to such methods. For instance, it is often inconvenient to monopolize the use of a general purpose laboratory laser for a task which could be performed by a less expensive, simpler device. Further, the finite filament dimensions of incandescent lamps produce an uneven luminous intensity distribution in an image beam. Also, the luminous output of such lamps varies nonlinearly with filament current.

Light-emitting diodes (LED) are another candidate. The light radiated by these lamps is typically either red, green, yellow, or orange. They require only small amounts of input power, usually 30 mA at less than 2 V. Luminous intensities range from 1.0–10.0 mcd. Their operating temperature is low enough to be cool to the touch, and the LED housings are such that they can be easily inserted into small (1/4-in. diam) mounting holes in panels or other thin plates.

Most commercially available two-lead LED "display lamps" have an epoxy-drop lens above the active element. Their properties as a point source emitter are discussed by Wunderlich *et al.*[1] Sometimes, however, the presence of this lens complicates collimation and in some cases makes it impossible due to extreme surface deformation. The optical characteristics of these lenses usually vary from diode to diode, and simple arguments show that in most cases they produce a virtual image of the source.

By altering the LED structure however, these problems can be overcome.

Using a serrated-edge knife, the epoxy lens can be cut off the diode approximately 1/32 inch or so above the diode active area. Care must be taken not to expose or otherwise damage the diode active area during cutting; further, the cut must be made perpendicular to the diode axis. Any large surface irregularities due to the cutting process can then be gently filed down until the resultant surface is flat to the touch. The surface will be cloudy because of the scratches on the remaining epoxy. It can be polished to transparency however, by carefully rubbing it on a smooth sheet of very fine grain finishing paper (placed on a flat working surface) which has been lubricated with a couple of drops of mineral oil.

It is very easy in this way to obtain a point source emitter whose beam can be easily collimated. Depending on the structure of the diode active element, the image may be composed of the separately magnified emitter components; however appropriate masking or very slight beam defocusing will provide the user with a beam of uniform intensity.

I would like to thank Professor Rogers Ritter for his helpful discussion and the NSF and National Institutes of Health for financial assistance under Grants No. PHY78-03208 and GM1682-08, respectively.

[1] F. J. Wunderlich, D. E. Shaw, and H. J. Hones, Am. J. Phys. 45, 106 (1977).

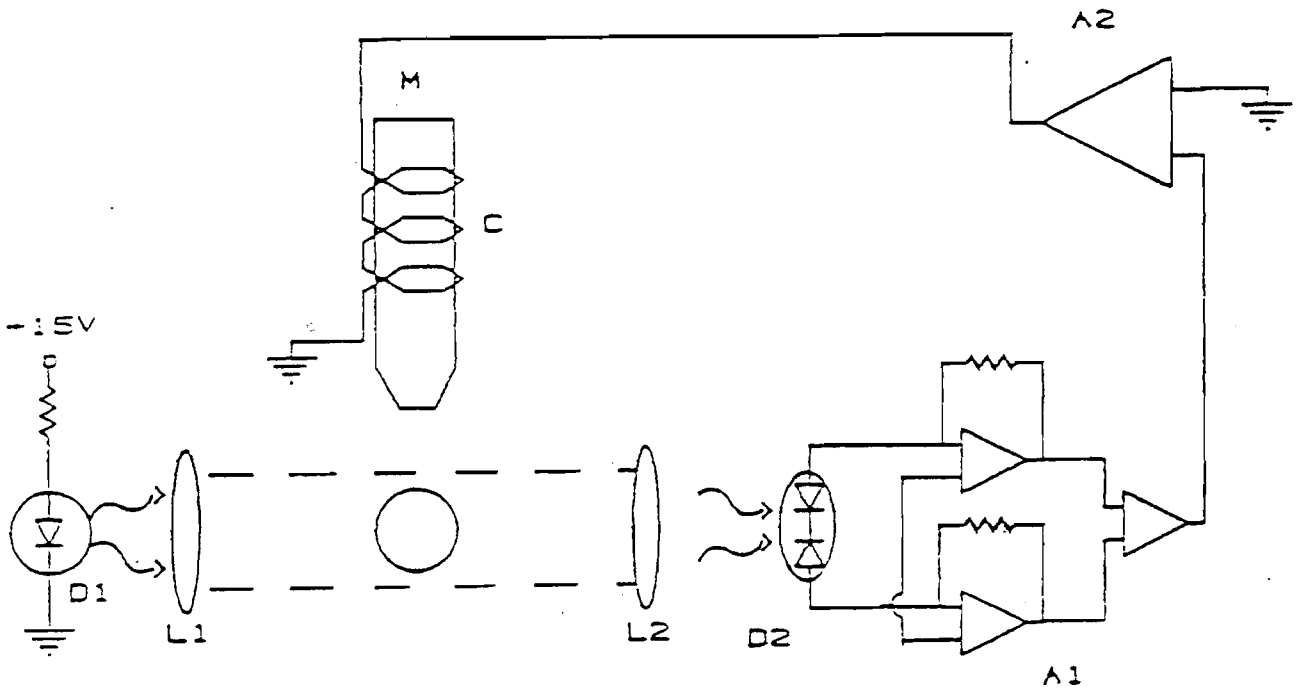


Figure 1. The block diagram for the operation of a magnetic suspension system using a split-cell photodetector.

- 19 -

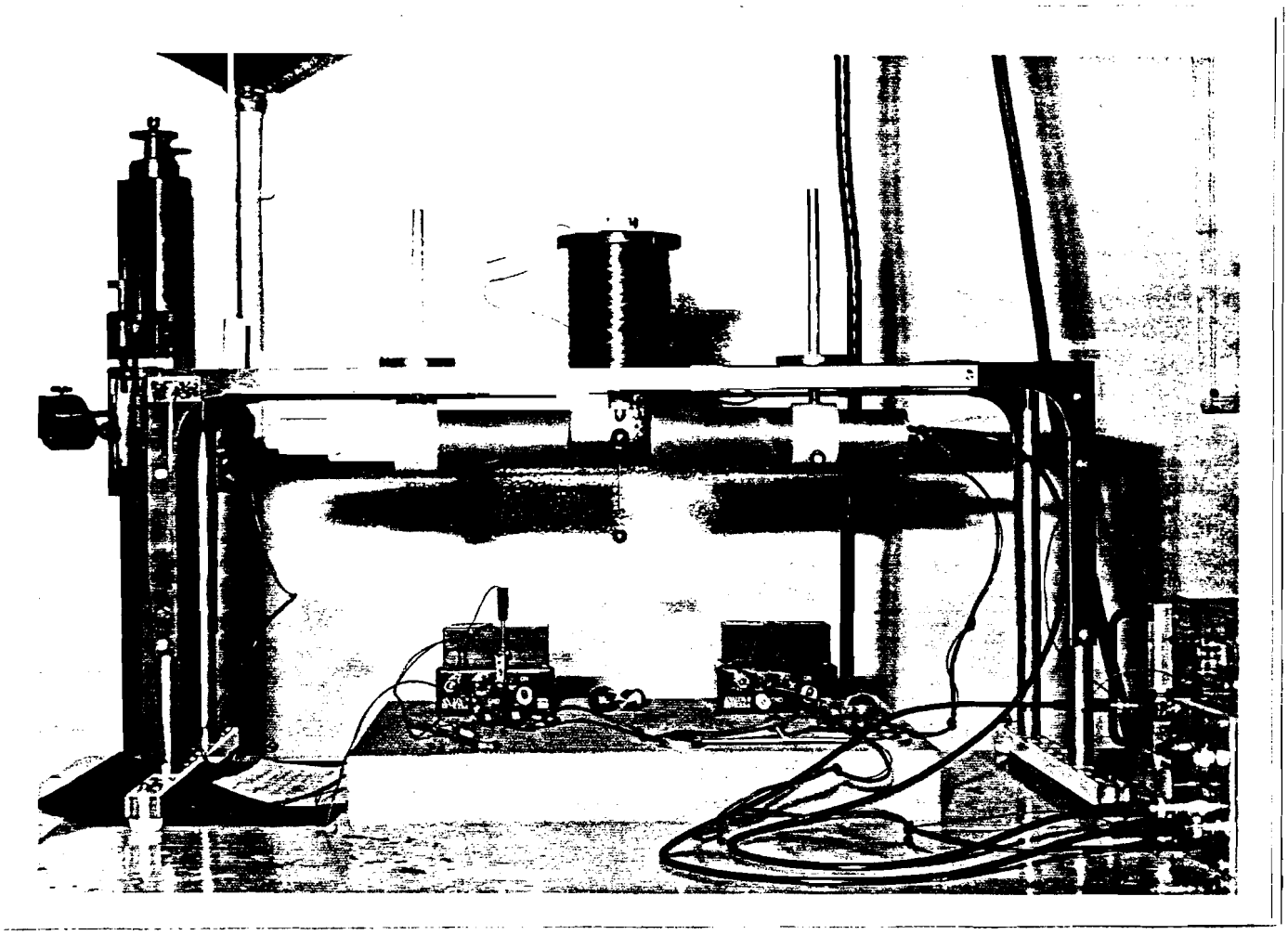

Figure 2. An overall view of BIPM-1 in operation, showing full mechanical detail.

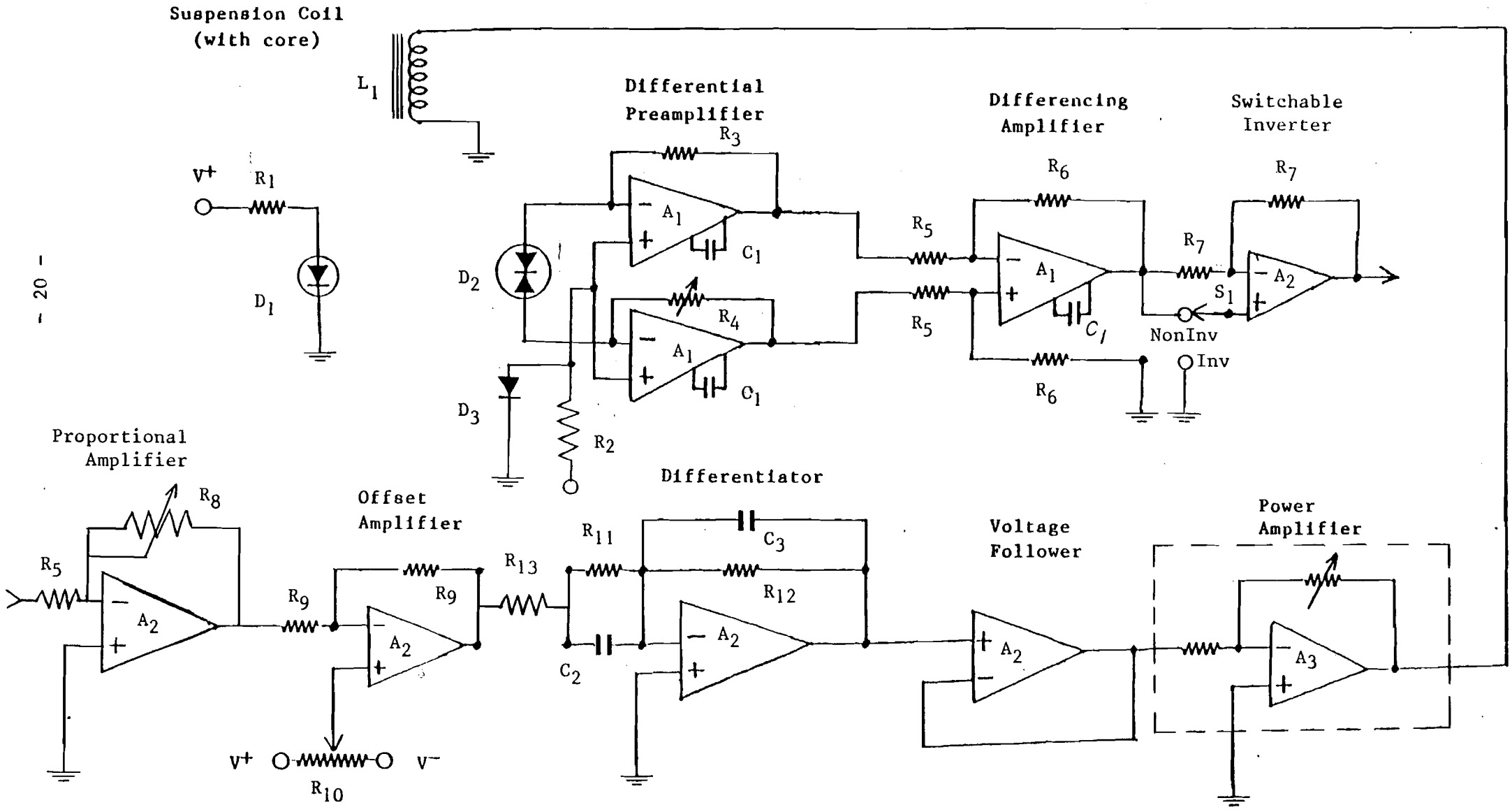


Figure 3. The schematic diagram of the suspension's electronics, with a complete parts list on the following page.

Parts List for the Electronics Circuitry

| Code | Component | Part Number/ Component Value | Manufacturer | Quantity |
|---|---|---|---|---|
| $A_1$ | op amp | LM308AN | National semiconductor | 3 |
| $A_2$ | op amp | CA741CE | RCA | 5 |
| $A_3$ | power amplifier | BOP 36-6M | Kepko, Inc. | 1 |
| $C_1$ | capacitor | 20 pF | Centralab | 3 |
| $C_2$ | capacitor | 2.2 μF | EFD | 1 |
| $C_3$ | capacitor | 2.2 nF | EFD | 1 |
| $D_1$ | LED | MV 5752 | Monsanto | 1 |
| $D_2$ | Quadrent Photodetector | SD-380-23-21-051 | Silicon Detector Corp. | 1 |
| $D_3$ | zenar diode | 137A | ECG | 1 |
| $L_1$ | coil with iron core | 0.85 H | BIPM | 1 |
| $R_1$ | 5 W power resistor | 500 Ω | SERNICE | 1 |
| $R_2$ | 1/4 W Resistor | 10 kΩ | Allen-Bradley | 1 |
| $R_3$ | 1/8 W Resistor | 470 kΩ | Allen-Bradley | 1 |
| $R_4$ | Potentiometer | 470 kΩ | SERNICE | 1 |
| $R_5$ | 1/8 W Resistor | 1 kΩ | Allen-Bradley | 3 |
| $R_6$ | 1/8 W Resistor | 22 kΩ | Allen-Bradley | 2 |
| $R_7$ | 1/8 W Resistor | 10 kΩ | Allen-Bradley | 2 |
| $R_8$ | Potentiometer | 22 kΩ | MCB | 1 |
| $R_9$ | 1/8 W Resistor | 10 kΩ | TRW/IRC | 2 |
| $R_{10}$ | Potentiometer | 10 kΩ | MCB | 1 |
| $R_{11}$ | 1/8 W Resistor | 13 kΩ | Allen-Bradley | 1 |
| $R_{12}$ | 1/8 W Resistor | 22 kΩ | Allen-Bradley | 1 |
| $R_{13}$ | 1/8 W Resistor | 47 Ω | Allen-Bradley | 1 |
| $S_1$ | SPST Switch | 1-2-3 | SECMB | 1 |

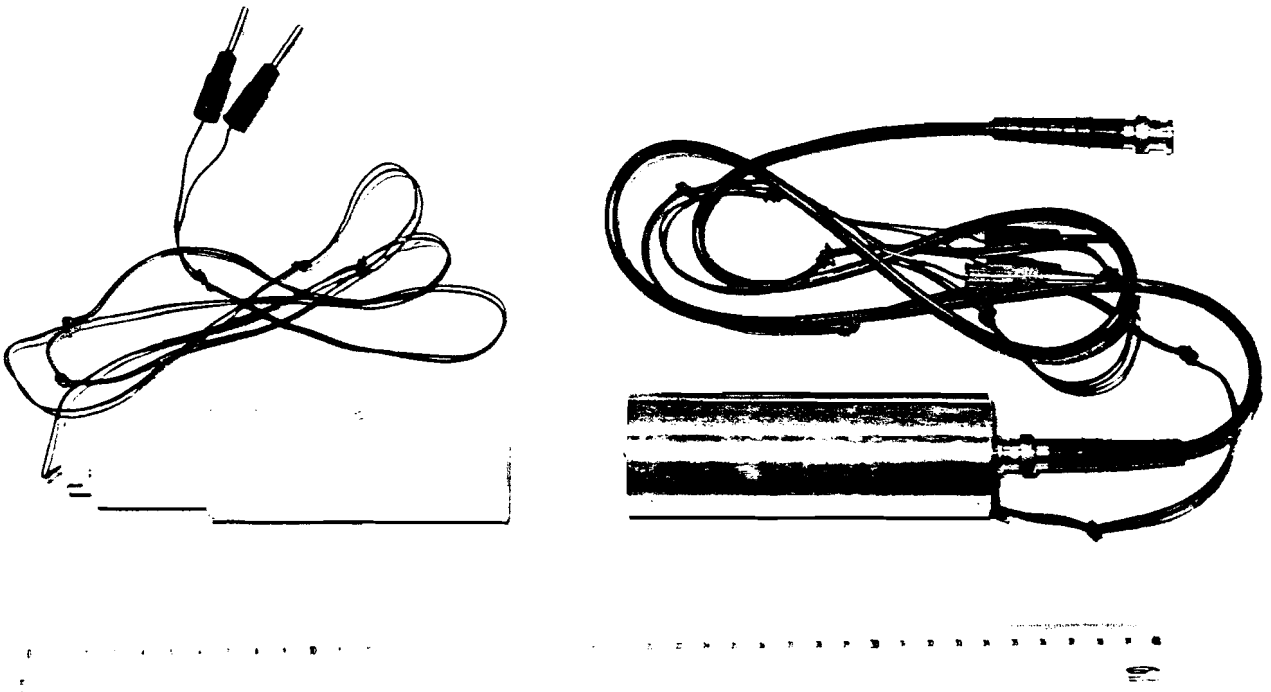

Figure 4. The tubes housing the LED and lens (on the left) and the photodetector and preamplifier (on the right).

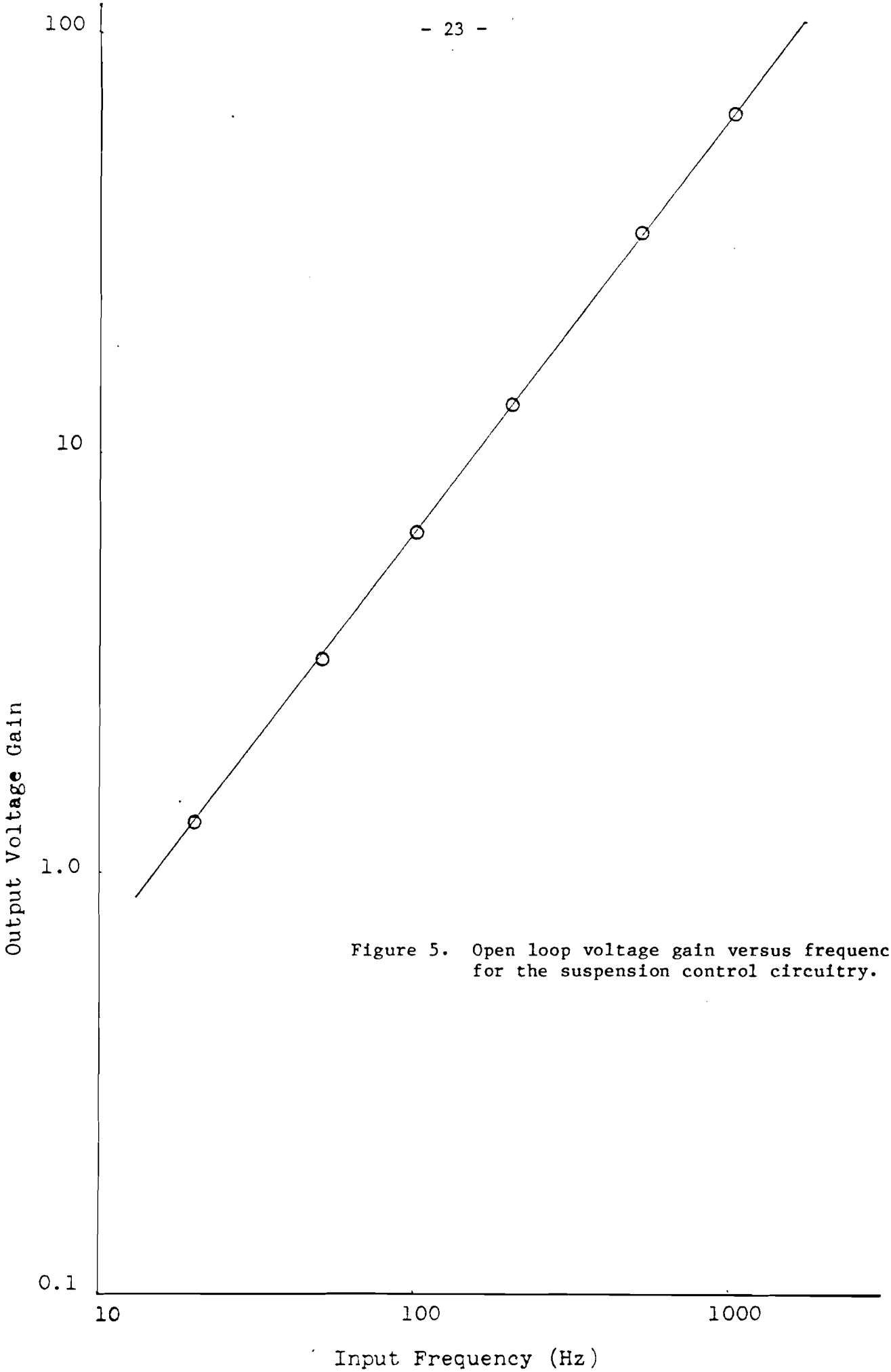


Figure 5. Open loop voltage gain versus frequency for the suspension control circuitry.

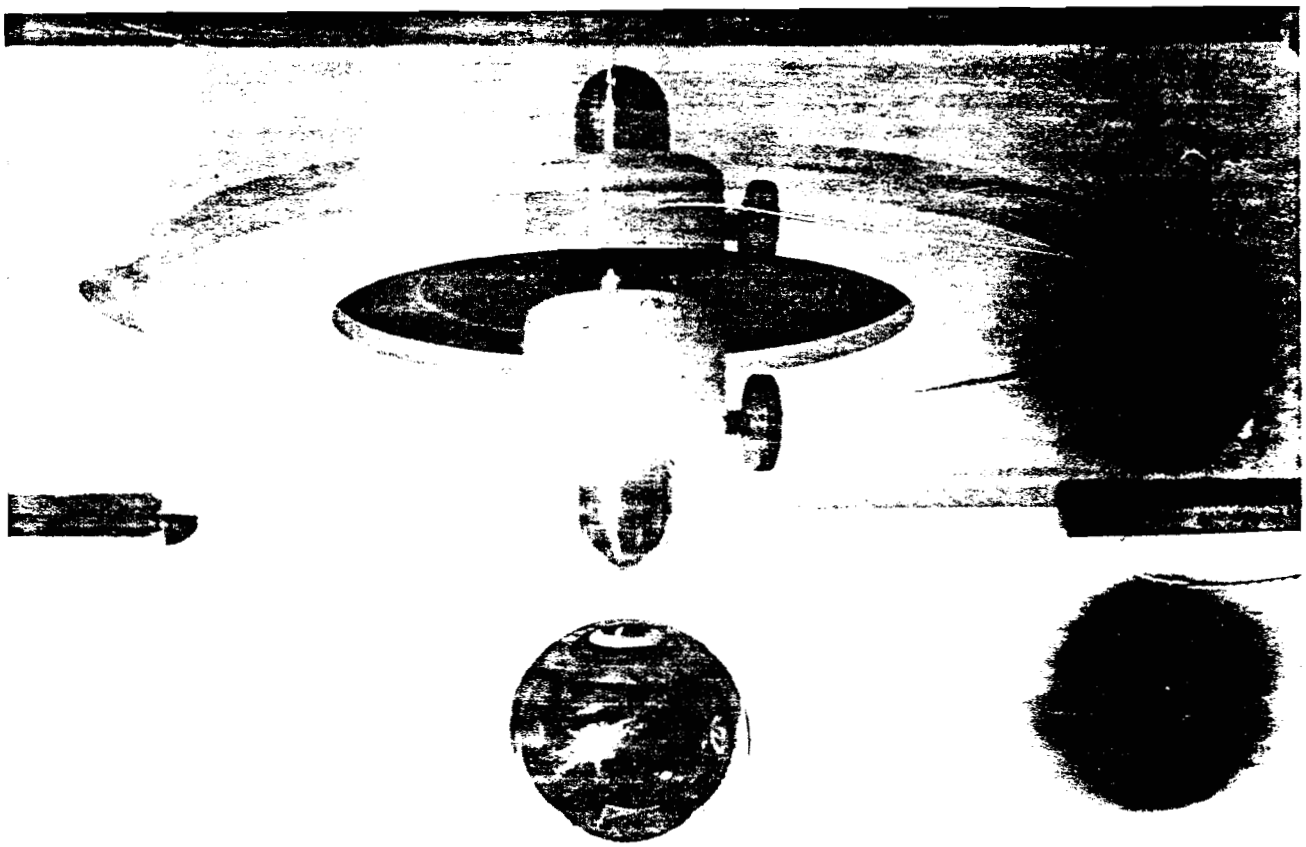

Figure 6. A magnetically suspended steel ball with a mass of about 100 g.

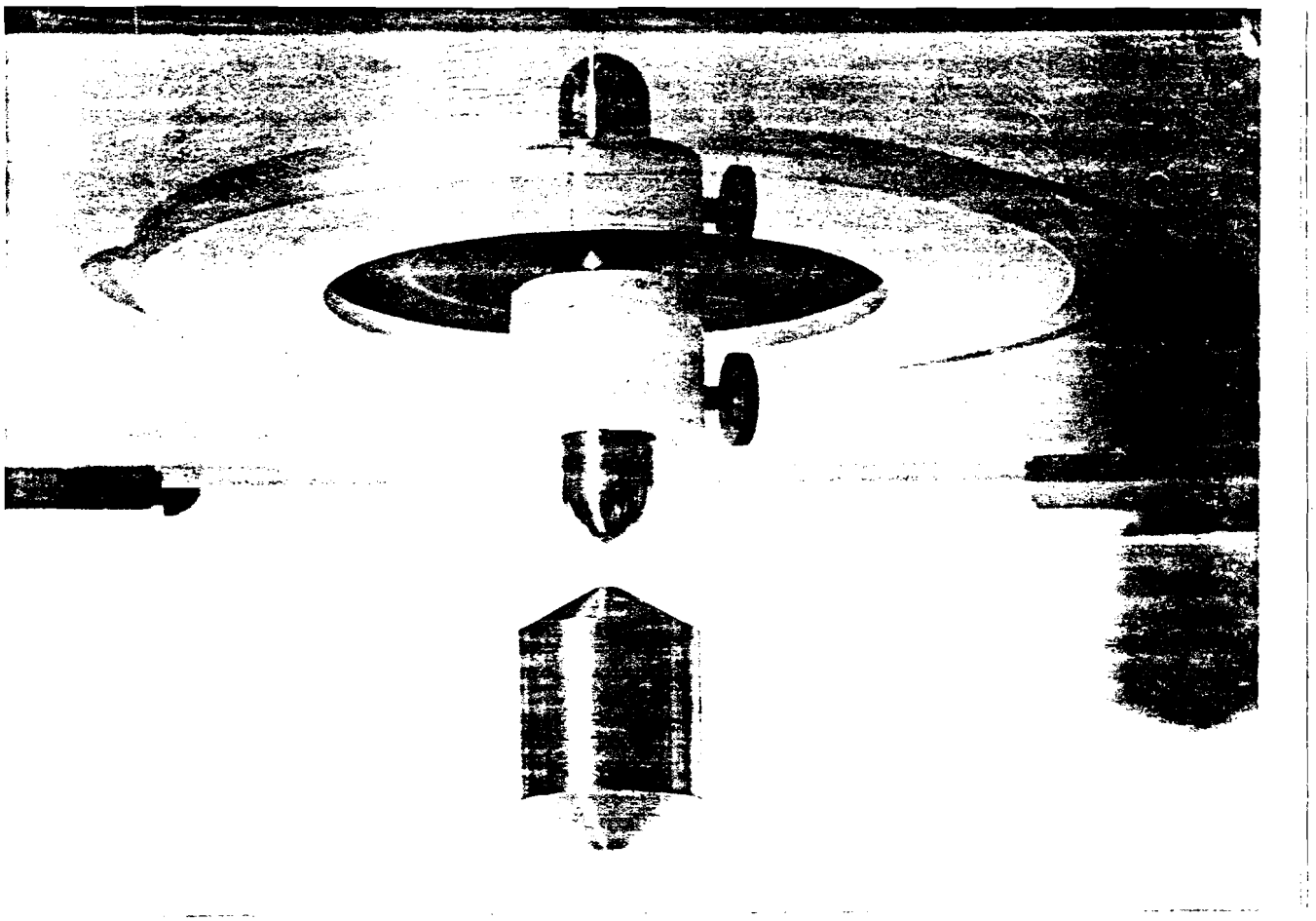

Figure 7. A magnetically suspended cylinder (with tapered ends) of mass about 100 g.

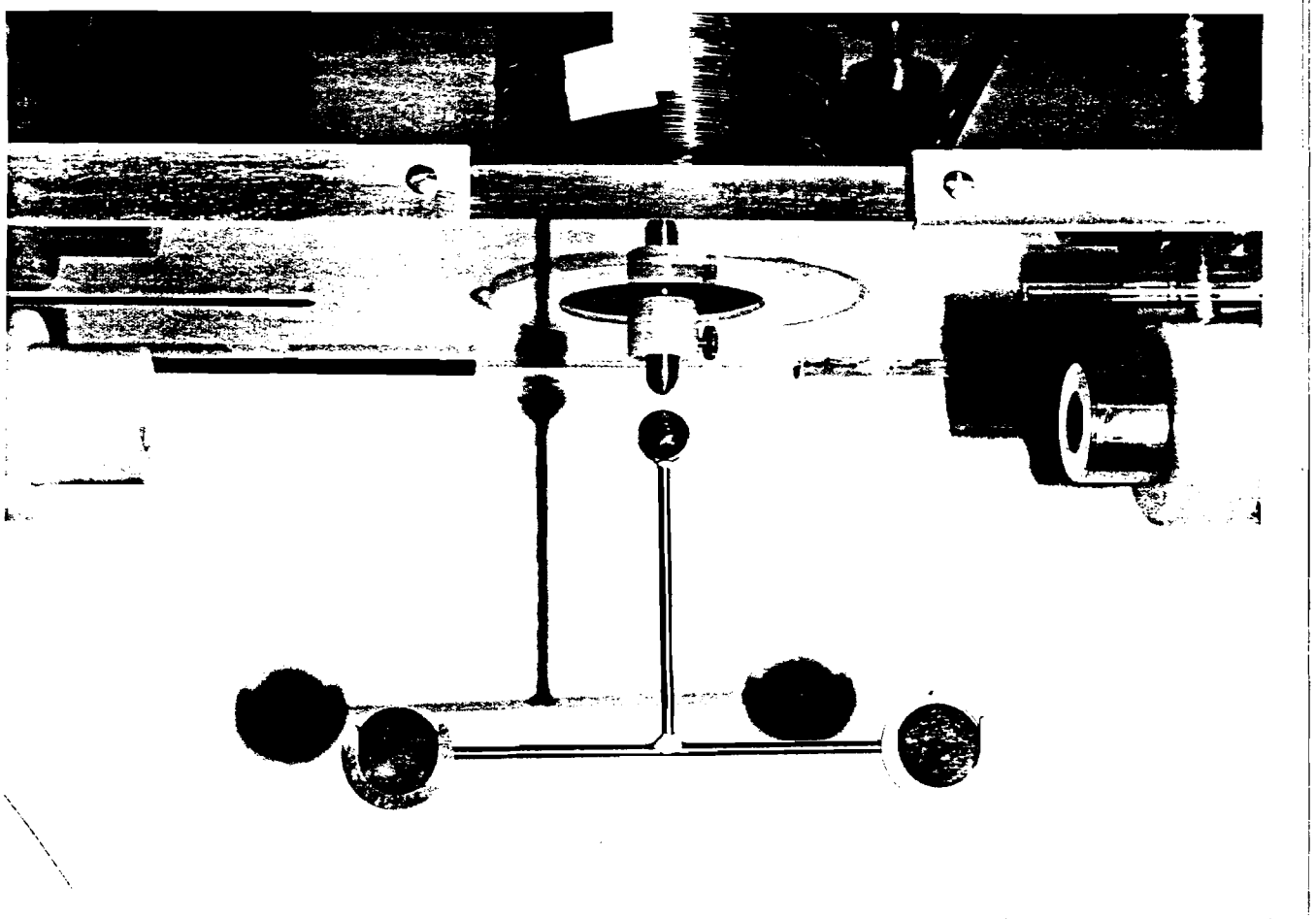

Figure 8. A magnetically suspended "inverse Tee" used as the detector in a new absolute measurement of laser output power.

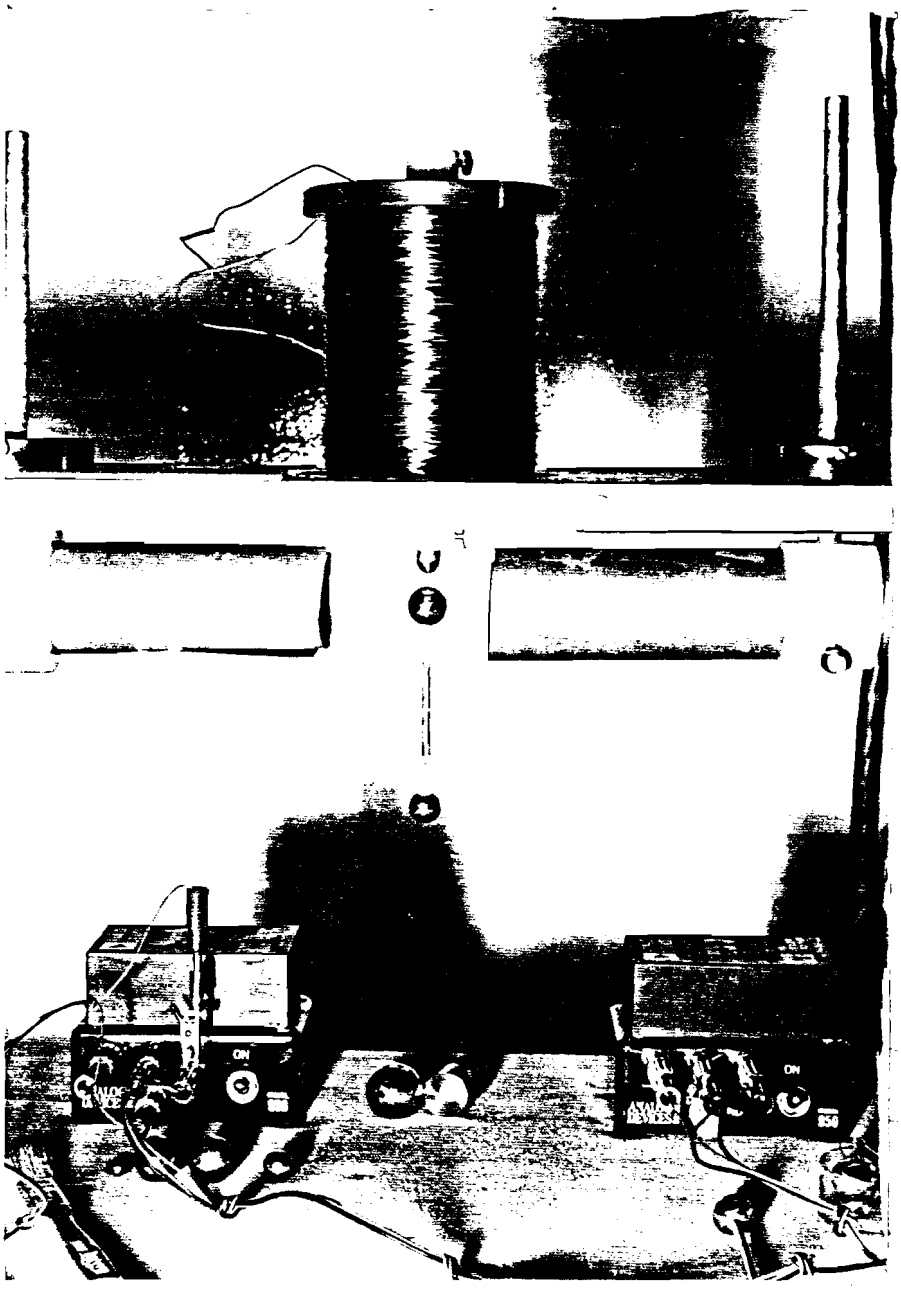

Figure 9. Coupled oscillators, in magnetic suspension, for possible use in an ultra-low frequency vibration isolation system.